ARTICLE

A Physiologically-Based Pharmacokinetic Model for the Prediction of "Half-Life Extension" and "Catch and Release" Monoclonal Antibody Pharmacokinetics

Hannah M. Jones[1], John Tolsma[2], Zhiwei Zhang[2], Paul Jasper[2], Haobin Luo[2], Gregory L. Weber[1], Katherine Wright[3], Joel Bard[1], Robert Bell[4], Dean Messing[1], Kerry Kelleher[1], Nicole Piche-Nicholas[1] and Robert Webster[1,*]

Monoclonal antibodies (mAbs) can be engineered to have "extended half-life" and "catch and release" properties to improve target coverage. We have developed a mAb physiologically-based pharmacokinetic model that describes intracellular trafficking, neonatal Fc receptor (FcRn) recycling, and nonspecific clearance of mAbs. We extended this model to capture target binding as a function of target affinity, expression, and turnover. For mAbs engineered to have an extended half-life, the model was able to accurately predict the terminal half-life (82% within 2-fold error of the observed value) in the human FcRn transgenic (Tg32) homozygous mouse and human. The model also accurately captures the trend in pharmacokinetic and target coverage data for a set of mAbs with differing catch and release properties in the Tg32 mouse. The mechanistic nature of this model allows us to explore different engineering techniques early in drug discovery, potentially expanding the number of "druggable" targets.

Study Highlights

WHAT IS THE CURRENT KNOWLEDGE ON THE TOPIC?
☑ Several groups have engineered antibodies to have extended half-life and catch and release properties. There are no examples of using *in vitro* data to describe these properties in a modeling framework to predict *in vivo* pharmacokinetics (PK) and target coverage.

WHAT QUESTION DID THIS STUDY ADDRESS?
☑ This work seeks to understand whether *in vitro* data can be used in a physiologically-based PK model framework to predict the *in vivo* PK for antibodies engineered to have extended half-life and catch and release properties.

WHAT DOES THIS STUDY ADD TO OUR KNOWLEDGE?
☑ This work shows that for antibodies engineered to have extended half-life and catch and release properties, *in vivo* PK and target coverage can be predicted accurately.

HOW MIGHT THIS CHANGE DRUG DISCOVERY, DEVELOPMENT, AND/OR THERAPEUTICS?
☑ This approach offers the potential to explore different engineering techniques early in drug discovery potentially expanding the number of druggable targets.

Over recent years, monoclonal antibodies (mAbs) have represented a growing class of therapeutics[1,2] with over 50 mAbs currently in late-stage clinical studies.[3] This success is due to their high affinity and specificity for the therapeutic target of interest together with their long serum terminal half-life ($t_{1/2}$).

Dosing regimen is affected by the pharmacokinetics (PK) of the mAbs, the affinity of the mAbs for the target of interest, as well as the properties of the target (levels and turnover). In early drug discovery, feasibility analyses are often performed to determine, based on the properties of the target, whether the target is "druggable." Recently, Farrokhi *et al*.[4] evaluated the feasibility of osteopontin neutralization; PK/pharmacodynamic (PD) modeling revealed that the turnover

of osteopontin (11 minutes) was too fast to achieve sustained suppression of osteopontin in a clinical setting. In addition, omalizumab is no longer indicated for patients with very high baseline immunoglobulin E concentrations, due to the high dose required to reduce free immunoglobulin E back to healthy levels[5] indicating the importance of target properties. In some cases, it may be possible to "rescue" such targets by developing mAbs engineered to have "$t_{1/2}$ extension" or "catch and release" properties to improve PK and target coverage.

The pH-dependent binding of mAbs to the neonatal Fc receptor (FcRn) in the acidic environment (pH 6) of the endosome and release from FcRn at the cell surface (pH 7.4) is key to protecting mAbs from lysosomal proteolytic degradation.

[1]BioMedicine Design, Pfizer Worldwide R&D, Cambridge, Massachusetts, USA; [2]RES Group Inc., Needham, Massachusetts, USA; [3]BioMedicine Design, Pfizer Worldwide R&D, Andover, Massachusetts, USA; [4]Rare Disease Research Unit, Pfizer Worldwide R&D, Cambridge, Massachusetts, USA. *Correspondence: Robert Webster (rob.webster@pfizer.com)

Selectively increasing the binding affinity of the Fc region of the mAb to FcRn at pH 6 alone has been shown to increase the $t_{1/2}$ of several mAbs in the clinical setting, thus improving target coverage. Specifically, mutations in three amino acids (M252Y, S254T, and T256E (YTE)) within the Fc region of motavizumab and MEDI4893[6,7] and mutations in two amino acids (M428L and N434S (LS)) within the Fc region of VRC01[8,9] resulted in a 4-fold to 5-fold increase in $t_{1/2}$ compared with their wild-type (WT) pairs. Borrok *et al.*[10] studied a panel of mAb variants and revealed the importance of not only affinity to FcRn at pH 6 but also affinity to FcRn at pH 7.4.

Another approach to optimize mAb target coverage is using catch and release mAbs.[11,12] Briefly, these engineered mAbs can "catch" (bind) the target protein of interest at neutral pH and "release" (unbind) the target protein within the acidic environment of the endosome. This allows the target protein to be degraded in the lysosome and the recycling of the FcRn bound mAb back to the cell surface where it is released and free to bind more target proteins. These mAbs commonly use "histidine switching" to generate pH-dependent release from target, wherein site-directed mutagenesis is applied to insert histidine residues at sites where a positive charge will destabilize the mAb-target interaction.[13] In addition, "sweeping" mAbs that have catch and release properties have also been engineered to have increased affinity to FcRn at neutral pH to enable enhanced uptake into the endosome.[14]

We have previously developed a physiologically-based PK (PBPK) model that we can use prospectively early in the drug discovery process to select mAbs with optimal PK and, therefore, the best chance of clinical success.[15] We expanded the Shah and Betts[16] model to include a mechanistic description of pH dependent FcRn-mAb dynamics within the endothelial cell compartment and have included an additional clearance (CL) mechanism to describe nonspecific interactions within each organ compartment using affinity-capture self-interaction nanoparticle spectroscopy (AC-SINS) data[17] (see **Supplementary Materials Text S1**). The first aim of this work is to test the ability of this model to predict the effect of "$t_{1/2}$ extension" mutations (LS and YTE) on PK using a series of WT and $t_{1/2}$ extension pairs. Second, we extend the model to incorporate target binding kinetics and explore its ability to predict the effect of catch and release and sweeping mutations on the PKs and target coverage of the extracellular form of a highly expressed soluble protein, cyclophilin A (CypA).

METHODS
Antibody selection
For the $t_{1/2}$ extension work, several internal and literature mAbs were used. Three internal WT and $t_{1/2}$ extension (LS) pairs were selected (mAb1 (WT), mAb1 (LS), mAb2 (WT), mAb2 (LS), mAb3 (WT), and mAb3 (LS)) based on availability of *in vivo* PK data in the human FcRn transgenic (Tg32) mouse model. In addition, motavizumab (WT and YTE), VRC01 (WT and LS) and MEDI4893 (YTE) were selected due to the availability of clinical PK data from the literature.[6–9]

For the catch and release and sweeping work, several internal mAbs were used. MAb0109 was selected as a control and binds tightly to the target of interest, CypA and demonstrates "typical" binding affinities to FcRn at pH 6 and 7.4. MAb0117 and mAb0128 were engineered to have catch and release properties. MAb0222 was engineered from mAb0117, it retains the catch and release properties but also includes a mutation described by ref. 14 to enhance FcRn binding at pH 6 and 7.4 (sweeping mAb). MAb0223 was engineered from mAb0117 to include the LS $t_{1/2}$ extension mutation.

In vivo Tg32 mouse and human PK and PK/PD studies
In vivo PK studies to support the $t_{1/2}$ extension modeling were conducted in the Tg32 homozygous mouse model as described by Avery *et al.*[18] for mAbs 1–3 (WT and LS). In brief, mAbs were dosed intravenously at a saturating dose of 5 mg/kg. A total of 4–6 mice were evaluated for each mAb. Serum samples were analyzed as described previously.[18] PK parameters (CL, volume of distribution at steady state (V_{ss}), and $t_{1/2}$) were derived from individual animal data using noncompartmental analysis in Phoenix WinNonlin (version 6.3; Certara L.P. (Pharsight). A small proportion (< 10%) of plasma concentration-time profiles showed a sharp drop in exposure (presumed due to antidrug antibodies) and were excluded. Below the limit of quantification samples were set as 0 for data analysis. All Tg32 mouse studies were conducted at Pfizer. Procedures performed on animals were in accordance with regulations and established guidelines and were reviewed and approved by Pfizer's Institutional Animal Care and Use Committee. Clinical PK data for motavizumab (WT and YTE), VRC01 (WT and LS), and MEDI4893 (YTE) were obtained from the literature.[6–9] Data were typically available over a dose range and subsequently averaged.

In vivo PK/PD studies to support the catch and release and sweeping modeling were conducted with mAbs 0109, 0117, 0222, 0223, and 0128 in the Tg32 homozygous mouse model as described above using single intravenous dose of 100 mg/kg. Serum samples were also analyzed for total CypA (free and mAb-bound CypA) levels using an immunoaffinity liquid-chromatography tandem mass spectrometry assay (see **Supplementary Materials Text S1**).

In vitro data (AC-SINS, FcRn affinity, and CypA affinity)
AC-SINS data were generated for all mAbs studied as described by Jones *et al.*[15] AC-SINS values were not available for motavizumab (WT and YTE), VRC01 (WT and LS), and MEDI4893 (YTE) and were assumed to be 0 (based on WT observed $t_{1/2}$ values being in the "well-behaved" mAb range).

FcRn affinity constant (k_d) values at pH 6 and 7.4 (if measurable) were generated for all internal mAbs studied, as described by ref. 15 All k_d values at pH 7.4 were fixed at $220 \times k_d$ at pH 6 for WT mAbs as reported by ref. 15 and fixed at 154,000 nM for LS and YTE mAbs (default pH 7.4 value reported by ref. 15). For motavizumab (WT) the k_d at pH 6 was assumed to be 700 nM,[15] and for motavizumab (YTE) it was scaled using the reported k_d pH 6 ratio between WT and YTE.[10] For VRC01 (WT and LS) the same approach was applied as for motavizumab but using the reported k_d pH 6 ratio from ref. 19 For MEDI4893 (YTE), the k_d value at pH 6 was assumed the same as motavizumab (YTE). The binding on-rate (k_{on}) values at pH 6 (8.06E + 7 1/(M*h)) were taken from ref. 16. The k_{on} values at pH 7.4 (3.8E + 6 1/(M*h)) were assumed to be 21× slower than at pH 6.[20,21] The binding off-rate (k_{off}) was calculated from k_{on} and k_d.

CypA k_d and k_{on} values were determined at both pH 6 and pH 7.4 using surface plasmon resonance. The procedure was similar to that described for FcRn by ref. 18. CypA was flowed as the analyte, against the anti-human Fc captured (GE Healthcare, BR-1008-39) anti-CypA mAbs. k_{off} was calculated from k_{on} and k_d.

All *in vitro* data are shown in **Tables 1 and 2**.

Model description

The PBPK model described previously[15] was used in this work. This model was parameterized for both the Tg32 mouse and human. Briefly, the model contains a plasma compartment and 15 tissue compartments. Each tissue compartment is subdivided into a vascular compartment, a vascular-side membrane compartment, an endothelial cell compartment, an interstitial-side membrane compartment, an interstitial fluid compartment, and a cellular space compartment. Within the endothelial cell compartment, a single cell mechanistic model of FcRn-mAb dynamics has been constructed. The transit of mAb around the body and between organs is mediated via plasma flow into tissues and then return via plasma flow except for the portion undergoing lymphatic drainage into a lymph node compartment, which then exits back into plasma. Both endogenous and exogenous IgG were modeled separately to account for any

competition for FcRn in the endosomal space. The FcRn mechanistic model operates within endothelial cells located in each organ. The model is composed of membrane proximal compartments for both apical (vascular side) and basolateral (interstitial side) membranes that are in rapid equilibrium with plasma and interstitial fluid and three well-mixed intracellular endosomal transit compartments, the early endosome (pH 7.4), sorting endosome (pH 6), and recycling endosome (pH 7.4). This allows explicit modeling of mAb-FcRn kinetics as a function of pH (6 and 7.4) and time. An additional nonspecific CL mechanism was included in each organ compartment as defined by AC-SINS data (see **Supplementary Materials**).

This model was extended for the purposes of the catch and release modeling to incorporate (i) binding between target and mAb, (ii) target synthesis and degradation, and (iii) handling of target-mAb complex distribution and CL. The target considered was extracellular soluble CypA. Target binding is assumed to occur in all tissues and all compartments in each tissue. Although the target is extracellular, we consider binding in intracellular compartments because target enters the cell both while bound to the mAb and in the fluid that enters by pinocytosis. We assume the target-mAb binding occurs with a ratio between target and mAb of 2:1 forming both partially bound (dimer)

Table 1 *In vitro* input parameters for half-life extension PBPK modeling

Species	mAbs	AC-SINS	k_d pH 6, nM	k_d pH 7.4 (nM)	Source
Tg32	mab1, WT	1	1,156	254,210	In-house
Tg32	mab1, LS	1	54	154,000	In-house
Tg32	mab2, WT	5	1,175	258,500	In-house
Tg32	mab2, LS	5	57	154,000	In-house
Tg32	mab3, WT	0	452	99,396	In-house
Tg32	mab3, LS	0	32	154,000	In-house
Human	Motavizumab, WT	0	700	154,000	Borrok et al., 2015[10]
Human	Motavizumab, YTE	0	103	154,000	Borrok et al., 2015[10]
Human	VRC01, WT	0	700	154,000	Ko et al., 2014[19]
Human	VRC01, LS	0	58	154,000	Ko et al., 2014[19]
Human	MEDI4893, YTE	0	103	154,000	Borrok et al., 2015[10]

AC-SINS, affinity-capture self-interaction nanoparticle spectroscopy; k_d, affinity constant for neonatal Fc receptor (FcRn); LS, amino acids M428L and N434S; mAb, monoclonal antibody; PBPK, physiologically-based pharmacokinetics; Tg32 mouse, human FcRn transgenic (Tg32) mouse; WT, wild type; YTE, amino acids M252Y, S254T, and T256E.

Table 2 *In vitro* input parameters for catch and release PBPK modeling

Compound	mAb0109	mAb0117	mAb0222	mAb0223	mAb0128
CypA k_{on} pH 6, 1/M/s	1,830,000	231,000	236,000	121,000	2,870,000
CypA k_d pH 6, nM	0.15	564	1,144	1,102	3.8
CypA k_{on} pH 7.4, 1/M/s	2,190,000	18,800,000	26,800,000	15,500,000	3,670,000
CypA k_d pH 7.4, nM	0.09	3.2	2.7	3.1	0.42
Acid-switch ratio, pH 6/pH 7.4	1.6	179	425	355	9.1
FcRn k_d pH 6, nM	885	885	5.4	47	846
FcRn k_d pH 7.4, nM	194,645	194,645	175	154,000	186,089
FcRn k_d ratio, pH 7.4/pH 6	220	220	32	3,253	220
AC-SINS	3	4	6	3	7

AC-SINS, affinity-capture self-interaction nanoparticle spectroscopy; CypA, mouse recombinant cyclophilin A; FcRn, neonatal Fc receptor; k_d, affinity constant; k_{on}, on-rate; mAb, monoclonal antibody; PBPK, physiologically-based pharmacokinetics.

and fully bound (trimer) complexes. Therefore, k_{on} and k_{off} correspond to a single binding event between target and one site of the antibody. CypA k_d values at pH 6 and 7.4 are considered (**Table 2**). The values at pH 6 are used for binding within the acidified endosome compartment and the values at pH 7.4 are used in all other compartments of the model.

The molar flux expressions corresponding to this binding network are shown in Eqs. 1 and 2.

$$\text{Rate}_{dimer} = (2 \times k_{on} \times \text{mAb} \times \text{target} - k_{off} \times \text{dimer}) \times V \quad (1)$$

$$\text{Rate}_{trimer} = (k_{on} \times \text{dimer} \times \text{target} - 2 \times k_{off} \times \text{trimer}) \times V \quad (2)$$

where rate_{dimer} and rate_{trimer} are the production rates of dimer and trimer, respectively, with units of nmol/hour in the model. k_{on} and k_{off} have units of 1/nM/hour and 1/hour, respectively. Concentrations for the mAb, target, dimer, and trimer are nanomolar. Parameter V is the volume, in liters, for the compartment where the binding occurs. The factor of 2 in the expression for dimer production is due to having two binding sites on each mAb. The factor of 2 in the trimer production expression appears because one of two bound targets can fall off a trimer to form a dimer.

The model assumes the target is synthesized and cleared in plasma (Eq. 3).

$$V_{plasma} \times d\text{target}/dt = k_{syn,target} - k_{deg,target} \times \text{target} \\ \times V_{plasma} - \text{rate}_{dimer} - \text{rate}_{trimer} \quad (3)$$

where V_{plasma} is the volume of plasma, $k_{syn,target}$ is the synthesis rate of the target in nmol/hour, and $k_{deg,target}$ is the degradation rate of target in 1/hour. These parameter values ($k_{syn,target}$ and $k_{deg,target}$) were calculated from a previous PK/PD study in the Tg32 mouse and are described in detail in the **Supplementary Materials Text S1**.

Free mAb, dimer, and trimer are assumed to behave in an identical manner in terms of their CL and distribution properties. The PBPK model equations for free mAb, dimer, and trimer are identical, except for the addition of the appropriate binding rate expressions (Eqs. 1 and 2) for each species. Binding to FcRn at pH 6 and 7.4 is identical for free mAb, dimer, and trimer. Any target that dissociates from mAb complexes in the endosome at pH 6 (e.g., due to a pH-dependent change in affinity) is cleared, resulting in enhanced CL for catch and release mAbs.

Simulations

For the $t_{1/2}$ extension work, Tg32 mouse and human plasma concentration-time profiles were simulated for the different mAbs/doses studied using FcRn k_d values at pH 6 and 7.4 and AC-SINS data as input. Predicted vs. observed PK parameters were compared. A sensitivity analysis was also performed in Tg32 mouse and human to explore the relationship between FcRn k_d at pH 6 (1–10,000 nM) and pH 7.4 (100–1,000,000 nM) on $t_{1/2}$.

For the catch and release and sweeping work, simulations were performed using the extended PBPK model to predict Tg32 mouse mAb plasma exposure, total plasma CypA, and free plasma CypA levels after a single intravenous dose of 100 mg/kg using FcRn and CypA k_d values at pH 6 and 7.4 and AC-SINS data as input. Predicted vs. observed plasma concentration-time profiles were compared. In addition, using the human version of the model, a sensitivity analysis was performed to explore the relationship between CypA k_d at pH 7.4 (0.1–30 nM), CypA k_d at pH 6 vs. CypA k_d at pH 7.4 ratio ("acid switch" factor; 1–3,000) and predicted target coverage. This was done using both WT (700 nM at pH 6 and 154,000 nM at pH 7.4) and LS (32 nM at pH 6 and 154,000 nM at pH 7.4) FcRn binding affinities at a subcutaneous dose of 2 mg/kg every week.

Table 3 Observed vs. predicted PK parameters for half-life extension PBPK modelling

Species	mAbs	Terminal half-life		Clearance		Volume of distribution		Source
		Observed	Predicted	Observed	Predicted	Observed	Predicted	
Tg32	mab1, WT	12	9.5	0.34	0.39	121	124	In-house
Tg32	mab1, LS	15	41	0.20	0.093	93	131	In-house
Tg32	mab2, WT	14	7.5	0.22	0.60	101	148	In-house
Tg32	mab2, LS	19	33	0.11	0.14	74	162	In-house
Tg32	mab3, WT	15	21	0.22	0.17	106	123	In-house
Tg32	mab3, LS	19	45	0.17	0.080	106	125	In-house
Human	Motavizumab, WT	24	23	254	208	7.1	6.4	Robbie *et al.*, 2013[6]
Human	Motavizumab, YTE	82	60	53	80	6.3	6.7	Robbie *et al.*, 2013[6]
Human	VRC01, WT	15	23	384	208	NA	6.4	Ledgerwood *et al.*, 2015[8]
Human	VRC01, LS	71	68	36	70	NA	6.7	Gaudinski *et al.*, 2018[9]
Human	MEDI4893, YTE	90	60	46	80	5.7	6.7	Yu *et al.*, 2017[7]

Clearance units, mL/hr/kg for Tg32 mouse and mL/day for human; LS, amino acids M428L and N434S; mAb, monoclonal antibody; NA, not applicable; PBPK, physiologically-based pharmacokinetics; PK, pharmacokinetics; Terminal half-life units, days; Tg32 mouse, human FcRn transgenic (Tg32) mouse; Volume of distribution units, mL/kg for Tg32 mouse and liters for human; WT, wild type; YTE, amino acids M252Y, S254T, and T256E.

Target coverage was calculated from the free CypA levels relative to baseline.

Model coding

Model development, simulation, and control parameterization methods were implemented in J2 Dynamic Modeling and Optimization Software (RES Group, Needham, MA). The model code has also been implemented in Berkeley Madonna. The PBPK model code for PK only has been shared previously.[15] The PBPK model code including target can be found in the **Supplementary Materials Text S1**.

RESULTS

To explore the utility of the PBPK model framework to predict the PK of mAbs designed to have an extended $t_{1/2}$,
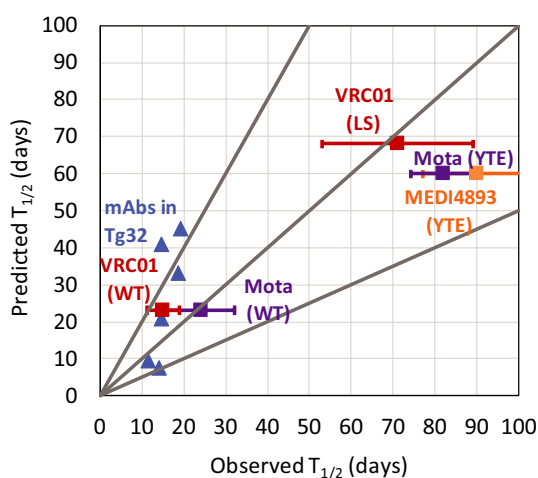
Figure 1 Predicted vs. observed $t_{1/2}$ for WT and half-life extended mAbs in Tg32 mouse and human. LS, amino acids M428L and N434S; mAb, monoclonal antibodies; Mota, motavizumab; $t_{1/2}$, terminal half-life; Tg32, human FcRn transgenic; WT, wild-type; YTE, amino acids M252Y, S254T, and T256E.

simulations of plasma concentration-time profiles were performed in Tg32 mouse and human. Predicted vs. observed PK parameters are shown in **Table 3**. In general, there is a good degree of prediction accuracy with 82%, 73%, and 89% of the predicted parameters being within 2-fold of the observed values for $t_{1/2}$, CL, and V_{ss}, respectively. More specifically, this prediction accuracy is illustrated for $t_{1/2}$ in **Figure 1**.

A sensitivity analysis was performed in Tg32 mouse and human to explore the relationship between FcRn k_d at pH 6 (1–10,000 nM) and pH 7.4 (100–1,000,000 nM) on $t_{1/2}$. This sensitivity analysis is shown in **Figure 2a,b** for Tg32 mouse and human, respectively. There appears to be an upper limit for $t_{1/2}$ of ~ 50 days and ~ 90 days in Tg32 mouse and human, respectively. As k_d at pH 6 becomes tighter and k_d at pH 7.4 becomes weaker, $t_{1/2}$ becomes longer and vice versa.

To explore the utility of the PBPK model framework to predict the PK and PK/PD of mAbs designed to have catch and release and sweeping properties, simulations were performed using the expanded PBPK model to predict Tg32 mouse mAb plasma exposure, total plasma CypA, and free plasma CypA levels. Predicted vs. observed plasma concentration-time profiles are shown in **Figure 3**. The model accurately captures the trend in these data. In terms of PK (**Figure 3a**), mAbs 0109, 0117, and 0128 have similar PK, whereas mAb0222 has worse exposure and mAb0223 has improved exposure. In terms of total plasma CypA levels (**Figure 3b**), mAb0109 has the largest increase in total plasma CypA levels, followed by mAb0128, 0223, 0117, and then 0222. Free plasma CypA levels were not measured in this study but based on the simulations (**Figure 3c**), the most sustained suppression of CypA was predicted with mAb0223, followed by 0117, 0128, 0109, and then 0222.

Using the human version of the model, a sensitivity analysis was performed to explore the relationship between CypA k_d at pH 7.4 (0.1–30 nM), acid switch factor (1–3,000) and predicted target coverage using both WT (700 nM at pH 6,

(a)

(b)
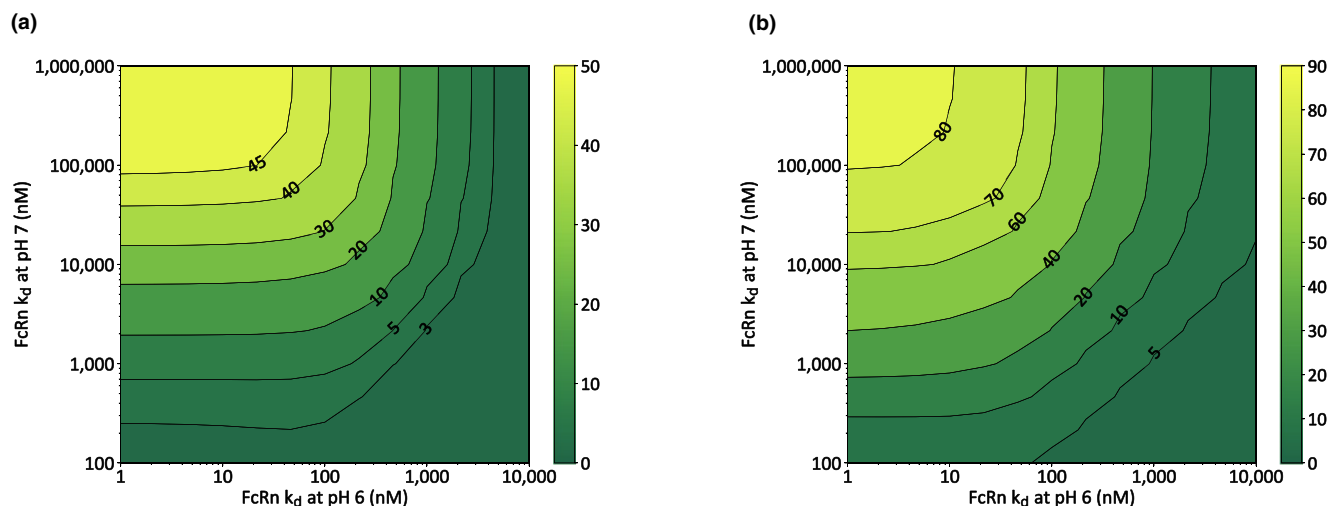
Figure 2 Heat map showing the relationship among neonatal Fc receptor (FcRn) affinity at pH 6 and FcRn affinity at pH 7.4 and terminal half-life contours (days). (**a**) Tg32 mouse and (**b**) human. k_d, affinity constant.

(a)

(b)

(c)
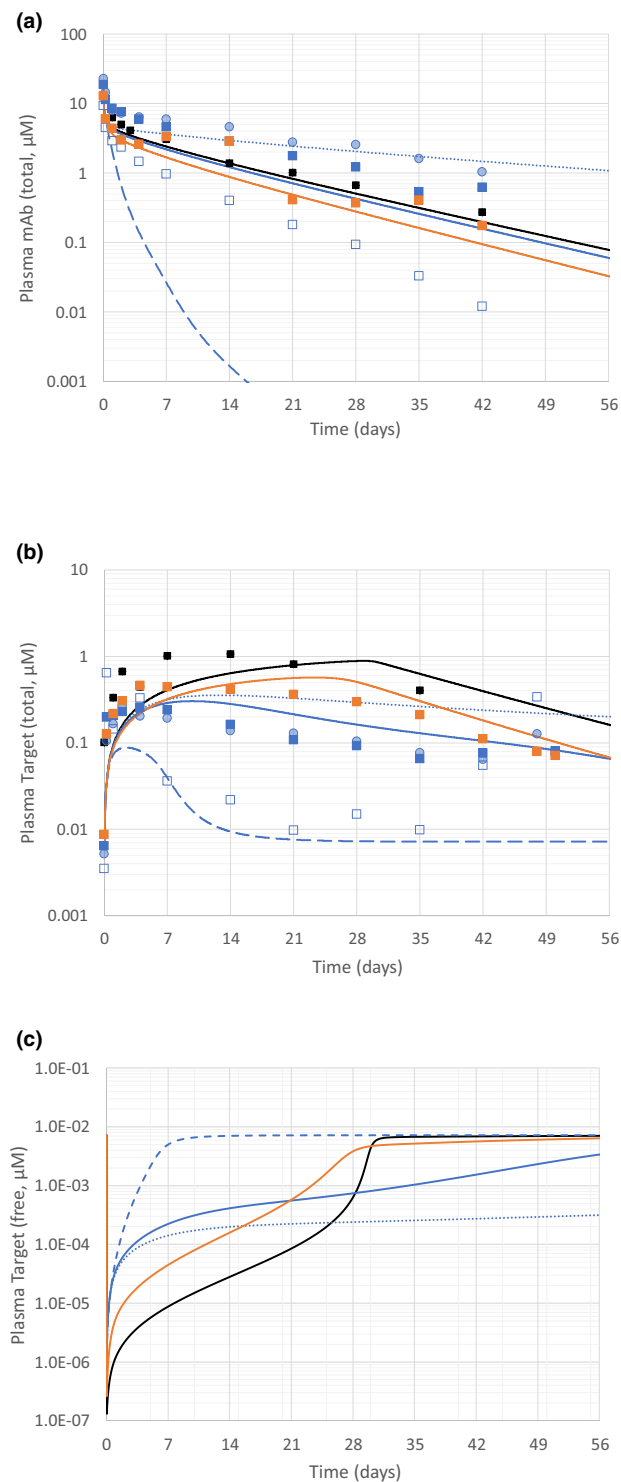
Figure 3 Observed vs. predicted plasma concentration-time profiles. (**a**) Observed vs. predicted monoclonal antibody (mAb) plasma concentration. (**b**) Observed vs. predicted total plasma cyclophilin A (CypA) concentration and (**c**) predicted free plasma CypA concentration. Black closed squares and solid line = mAb0109; blue closed squares and solid line = mAb0117; blue open squares and dashed line = mAb0222; blue shaded circles and dotted line = mAb0223; and orange closed squares and solid line = mAb0128.

154,000 nM at pH 7.4) and LS (32 nM at pH 6, 154,000 nM at pH 7.4) FcRn binding affinities. This heat map is shown in **Figure 4a,b** for WT and LS mAbs, respectively. These simulations indicate that in order to reduce plasma CypA levels by > 90% in humans, for a WT mAb, the CypA k_d at pH 7.4 and acid switch factor need to be 0.3–3 nM and 300–3,000, respectively. The criteria are slightly less stringent for LS mAbs, here, the CypA k_d at pH 7.4 and acid switch factor need to be 0.3–6 nM and 100–3,000, respectively.

DISCUSSION

There are a number of biotherapeutic PBPK models[16,20–27] that have been published that range in complexity. Recently, we published a PBPK model that utilizes *in vitro* data as input to predict *in vivo* PK *a priori*.[15] To improve dose level and regimen, various engineering technologies have been developed that extend PK and modify target binding properties of mAbs.[28,29] In this paper, we used our PBPK model to explore the predictability of PK and PD of mAbs engineered to have $t_{1/2}$ extension as well as catch and release and sweeping mutations.

Fc engineering that improves FcRn binding (7-fold (YTE) to 12-fold (LS)) in the endosome can give mAbs a longer $t_{1/2}$ by rescuing them more efficiently.[6–9] An important feature of this extended $t_{1/2}$ *in vivo* is the improvement in the pH 6 binding affinity while not effecting the affinity at pH 7.4. Our model was able to accurately predict the extended $t_{1/2}$ of these mAbs. There is a slight trend toward overprediction and underprediction of $t_{1/2}$ in Tg32 mouse and human, respectively (**Figure 1**). FcRn affinity at pH 7.4 is not measurable and represents one of the more uncertain parameters. For LS mAbs, this parameter is assumed the same as WT mAbs and the same across species. Sensitivity analysis indicates tighter pH 7.4 binding in Tg32 mouse (not human) improves this bias (**Figure 2**). However, as is shown in **Table 3**, there is generally a reasonable degree of prediction accuracy with 82%, 73%, and 89% of the predicted parameters being within 2-fold of the observed $t_{1/2}$, CL, and V_{ss} values, respectively. In comparison, the prediction accuracy was poorer using allometry from preclinical species (Tg32 mouse and cynomolgus monkey) for a limited number of mAbs (data not shown). These results indicate the potential of the PBPK model to explore PK prediction in early drug discovery for mAbs engineered to have improved FcRn recycling.

To better understand the pH dependence of FcRn binding, Borrok *et al.*[10] studied a panel of novel Fc mAb variants with high affinity binding at acidic pH with varying pH 7.4 affinities. PK studies in transgenic mice and cynomolgus monkey demonstrated that increased FcRn affinity at acidic pH results in an extended serum $t_{1/2}$ relative to the parental IgG. Interestingly, the results reveal an affinity threshold of neutral pH binding. Variants with pH 7.4 FcRn affinities below this threshold recycle efficiently and can exhibit increased serum persistence. Increasing neutral pH FcRn affinity beyond this threshold reduced serum persistence. This is assumed to be because the mAb remains bound to FcRn at neutral pH. Our model was also able to capture this

(a)

Acid-switch factor

k_d for CypA (nM)	1	3	10	30	100	300	1000	3000
0.1	17	18	21	28	42	69	97	99
0.3	20	23	29	42	70	92	97	98
0.6	23	27	38	56	81	93	96	97
1	25	31	44	65	84	92	95	96
3	30	38	54	69	82	87	89	90
6	29	38	52	66	76	81	82	83
10	27	36	50	62	70	74	75	75
30	20	29	40	47	51	53	53	54

(b)

Acid-switch factor

k_d for CypA (nM)	1	3	10	30	100	300	1000	3000
0.1	20	23	30	44	80	97	99	100
0.3	25	31	48	72	92	97	99	99
0.6	30	40	59	80	93	97	99	99
1	34	45	63	81	93	97	98	99
3	38	48	66	81	91	95	96	97
6	35	46	64	78	88	92	93	94
10	32	43	61	76	85	88	90	90
30	24	36	53	65	72	75	76	76

Figure 4 Heat map showing the predicted relationship between cyclophilin A (CypA) affinity at pH 7.4, acid switch factor and percent coverage of plasma CypA in human. (**a**) Wild-type monoclonal antibody and (**b**) half-life extended monoclonal antibody. k_d = affinity constant.

behavior (**Figure 2**). As k_d at pH 6 becomes tighter and k_d at pH 7.4 becomes weaker, $t_{1/2}$ becomes longer. However, as k_d at pH 7.4 become tighter, $t_{1/2}$ becomes shorter. In our model, this is captured by assuming that the FcRn-bound mAb is degraded at the rate of FcRn at neutral pH (11 hours).[30]

Engineering mAbs to make the antigen-binding pH-dependent can modulate antigen CL.[14] Such mAbs dissociate from the antigen in the acidic endosome allowing the antigen to be trafficked to the lysosome and degraded, whereas the mAb gets recycled back to the plasma via FcRn. By repeating this cycle, a pH-dependent antigen-binding mAb can bind to the target protein more than once. Igawa *et al.*[11] engineered an antibody against the IL-6 receptor (IL-6R), to rapidly dissociate from IL-6R within the endosome while maintaining its binding affinity to IL-6R in plasma. *In vivo* animal studies showed that this pH-dependent IL-6R binding resulted in enhanced lysosomal degradation of IL-6R and improved PK and duration of C-reactive protein inhibition. In addition, Chaparro–Riggers *et al.*[12] showed increased duration of cholesterol lowering with an antiproprotein convertase subtilisin kexin type 9 mAb engineered to have pH dependent binding. In our *in vivo* Tg32 mouse PK/PD studies (**Figure 3**), we were able to see a reduction in accumulation of total plasma CypA for mAbs engineered to have catch and release properties (mAbs 117 and 128) compared with WT mAbs (mAb109) indicating increased CypA degradation; this trend appears related to the acid switch factor. For mAb0223, which was engineered to have enhanced FcRn affinity at pH 6, improved PK and extended total coverage were observed *in vivo* and also modeled by the simulations. Using the model, we were also able to predict plasma CypA suppression, which was more sustained for those mAbs with high acid switch factors and improved FcRn affinity at

pH 6. The heat maps (**Figure 4**) illustrate there is a sweet spot for PK properties, CypA affinity and acid switch factor that in humans could lead to > 90% target coverage. Such analyses have the potential to be extremely informative in the design of mAbs with the greatest chance of success in the clinic.

It has been shown that the therapeutic potency of a pH-dependent antigen-binding mAb can be further enhanced by increasing their binding affinity to FcRn at neutral pH. Igawa *et al.* combined catch and release properties with enhanced FcRn binding at neutral pH.[14] They showed that, depending on the binding affinity to FcRn at neutral pH, that sweeping mAbs reduced soluble IL6R concentration 50-fold to 1,000-fold compared with a conventional mAb. Conversely, the $t_{1/2}$ of such mAbs was dramatically reduced. Our studies with a sweeping mAb (mAb 0222) showed an increase in total plasma CypA, however, the durability was poor. This trend has also been described by ref. 10 and our model was able to accurately capture this, as indicated previously. Mab 0222 has enhanced FcRn binding at pH 7.4 as well as catch and release properties. The enhanced FcRn binding at pH 7.4 leads to enhanced pinocytosis, which is thought to improve the catch and release efficiency. However, the enhanced FcRn binding at pH 7.4 also leads to poor PK and hence poor durability. The bound mAb-FcRn complex is assumed to clear at the rate of FcRn (11 hours). Given the clearance of this, mAb appears to be overpredicted (**Figure 3a**), the clearance of the complex may actually be slower than for FcRn alone.

Target-mediated CL and high antigen load (expression and turnover) can hamper the efficacy and dosing of many mAbs. The proposition that mAbs engineered to have improved binding to FcRn at acidic pH or pH-dependent

antigen binding may provide improvements in dosing level and frequency has been supported by the *in vivo* studies described in this work. We were able to show that our PBPK model framework could capture the effects of these engineering technologies on PK and PD profiles. This may provide an opportunity in early stages of drug discovery to explore previously deemed difficult targets.

Conflict of Interest. H.M.J., G.L.W., K.W., J.B., R.B., D.M., K.K., N.P.-N., and R.W. are (or were) employees of Pfizer Inc. when this work was conducted. J.T., Z.Z., P.J., and H.L. are employees of RES Group Inc., and conducted part of this work under contract with Pfizer Inc. All authors declared no other competing interests for this work.

Author Contributions. H.M.J. and J.T. wrote the manuscript. All authors (H.M.J., G.L.W., K.W., J.B., R.B., D.M., K.K., N.P.-N., R.W., J.T., Z.Z., P.J., and H.L.) designing the research, performed the research, and analyzed the data.

1. Dirks, N.L. & Meibohm, B. Population pharmacokinetics of therapeutic monoclonal antibodies. *Clin. Pharmacokinet.* **49**, 633–659 (2010).
2. Dostalek, M., Gardner, I., Gurbaxani, B.M., Rose, R.H. & Chetty, M. Pharmacokinetics, pharmacodynamics and physiologically-based pharmacokinetic modelling of monoclonal antibodies. *Clin. Pharmacokinet.* **52**, 83–124 (2013).
3. Kaplon, H. & Reichert, J.M. Antibodies to watch in 2018. *mAbs* **10**, 183–203 (2018).
4. Farrokhi, V., Chabot, J.R., Neubert, H. & Yang, Z. Assessing the feasibility of neutralizing osteopontin with various therapeutic antibody modalities. *Sci. Rep.* **8**, 7781 (2018).
5. Hochhaus, G. *et al.* Pharmacodynamics of omalizumab: implications for optimised dosing strategies and clinical efficacy in the treatment of allergic asthma. *Curr. Med. Res. Opin.* **19**, 491–499 (2003).
6. Robbie, G.J. *et al.* A novel investigational Fc-modified humanized monoclonal antibody, motavizumab-YTE, has an extended half-life in healthy adults. *Antimicrob. Agents Chemother.* **57**, 6147–6153 (2013).
7. Yu, X.Q. *et al.* Safety, tolerability, and pharmacokinetics of MEDI4893, an investigational, extended-half-life, anti-staphylococcus aureus alpha-toxin human monoclonal antibody, in healthy adults. *Antimicrob. Agents Chemother.* **61**, e01020-16 (2017).
8. Ledgerwood, J.E. *et al.* Safety, pharmacokinetics and neutralization of the broadly neutralizing HIV-1 human monoclonal antibody VRC01 in healthy adults. *Clin. Exp. Immunol.* **182**, 289–301 (2015).
9. Gaudinski, M.R. *et al.* Safety and pharmacokinetics of the Fc-modified HIV-1 human monoclonal antibody VRC01LS: a phase 1 open-label clinical trial in healthy adults. *PLoS Med.* **15**, e1002493 (2018).
10. Borrok, M.J. *et al.* pH-dependent binding engineering reveals an FcRn affinity threshold that governs IgG recycling. *J. Biol. Chem.* **290**, 4282–4290 (2015).
11. Igawa, T. *et al.* Antibody recycling by engineered pH-dependent antigen binding improves the duration of antigen neutralization. *Nat. Biotechnol.* **28**, 1203–1207 (2010).
12. Chaparro-Riggers, J. *et al.* Increasing serum half-life and extending cholesterol lowering in vivo by engineering antibody with pH-sensitive binding to PCSK9. *J. Biol. Chem.* **287**, 11090–11097 (2012).
13. Sarkar, C.A., Lowenhaupt, K., Horan, T., Boone, T.C., Tidor, B. & Lauffenburger, D.A. Rational cytokine design for increased lifetime and enhanced potency using pH-activated "histidine switching". *Nat. Biotechnol.* **20**, 908–913 (2002).
14. Igawa, T. *et al.* Engineered monoclonal antibody with novel antigen-sweeping activity in vivo. *PLoS One* **8**, e63236 (2013).
15. Jones, H.M. *et al.* A physiologically-based pharmacokinetic model for the prediction of monoclonal antibody pharmacokinetics from in vitro data. *CPT Pharmacometrics Syst. Pharmacol. 5, 738–747* (2019).
16. Shah, D.K. & Betts, A.M. Towards a platform PBPK model to characterize the plasma and tissue disposition of monoclonal antibodies in preclinical species and human. *J. Pharmacokinet. Pharmacodyn.* **39**, 67–86 (2012).
17. Liu, Y. *et al.* High-throughput screening for developability during early-stage antibody discovery using self-interaction nanoparticle spectroscopy. *mAbs* **6**, 483–492 (2014).
18. Avery, L.B. *et al.* Utility of a human FcRn transgenic mouse model in drug discovery for early assessment and prediction of human pharmacokinetics of monoclonal antibodies. *mAbs* **8**, 1064–1078 (2016).
19. Ko, S.Y. *et al.* Enhanced neonatal Fc receptor function improves protection against primate SHIV infection. *Nature* **514**, 642–645 (2014).
20. Chen, Y. & Balthasar, J.P. Evaluation of a catenary PBPK model for predicting the in vivo disposition of mAbs engineered for high-affinity binding to FcRn. *AAPS J.* **14**, 850–859 (2012).
21. Glassman, P.M. & Balthasar, J.P. Application of a catenary PBPK model to predict the disposition of "catch and release" anti-PCSK9 antibodies. *Int. J. Pharm.* **505**, 69–78 (2016).
22. Covell, D.G., Barbet, J., Holton, O.D., Black, C.D., Parker, R.J. & Weinstein, J.N. Pharmacokinetics of monoclonal immunoglobulin G1, F(ab')2, and Fab' in mice. *Cancer Res.* **46**, 3969–3978 (1986).
23. Baxter, L.T., Zhu, H., Mackensen, D.G. & Jain, R.K. Physiologically based pharmacokinetic model for specific and nonspecific monoclonal antibodies and fragments in normal tissues and human tumor xenografts in nude mice. *Cancer Res.* **54**, 1517–1528 (1994).
24. Ferl, G.Z., Wu, A.M. & DiStefano, J.J. 3rd. A predictive model of therapeutic monoclonal antibody dynamics and regulation by the neonatal Fc receptor (FcRn). *Ann. Biomed. Eng.* **33**, 1640–1652 (2005).
25. Garg, A. & Balthasar, J.P. Physiologically-based pharmacokinetic (PBPK) model to predict IgG tissue kinetics in wild-type and FcRn-knockout mice. *J. Pharmacokinet. Pharmacodyn.* **34**, 687–709 (2007).
26. Urva, S.R., Yang, V.C. & Balthasar JP. Physiologically based pharmacokinetic model for T84.66: a monoclonal anti-CEA antibody. *J. Pharm. Sci.* **99**, 1582–1600 (2010).
27. Glassman, P.M. & Balthasar, J.P. Physiologically based pharmacokinetic modeling to predict the clinical pharmacokinetics of monoclonal antibodies. *J. Pharmacokinet. Pharmacodyn.* **43**, 427–446 (2016).
28. Igawa, T., Tsunoda, H., Kuramochi, T., Sampei, Z., Ishii, S. & Hattori, K. Engineering the variable region of therapeutic IgG antibodies. *mAbs* **3**, 243–252 (2011).
29. Mimoto, F., Kuramochi, T., Katada, H., Igawa, T. & Hattori, K. Fc engineering to improve the function of therapeutic antibodies. *Curr. Pharm. Biotechnol.* **17**, 1298–1314 (2016).
30. Fan, Y.Y.F.V., Caiazzo, T., Wang, M., O'Hara, D.M. & Neubert, H. Human FcRn tissue expression profile and half-life in PBMCs. *Biomolecules* **9**, 373 (2019).